

Chimia 55 (2001) 165–170
© Neue Schweizerische Chemische Gesellschaft
ISSN 0009–4293

Structure-Mechanical Property Relationships in Engineering Polymers

Christopher J.G. Plummer* and Philippe Béguelin

Abstract: An overview is given of recent work in our laboratory aimed at exploring structure-mechanical property relationships in engineering polymers. This has involved both model systems and systems with direct relevance to practical industrial problems. However, the emphasis has always been on characterization in terms of intrinsic materials parameters and investigation of the underlying microdeformation mechanisms. Particular effort has gone into extending the range of test conditions over which fracture mechanics parameters such as K_{IC} or G_{IC} may be determined rigorously using simple geometries, up to and beyond speeds characteristic of impact tests. Alternative concepts such as the essential work of fracture have also been introduced in cases where linear elastic fracture mechanics fails to provide an adequate appreciation of the intrinsic behaviour of relatively ductile polymers. At the same time, microscopical techniques have been developed that give access to detailed information on the nature and extent of mechanically induced damage in specimens with different geometries, including bulk fracture specimens. In certain systems, this has made it possible to establish quantitative links between macroscopic fracture properties and microscopic parameters such as the number of covalent bonds crossing unit area of the crack plane.

Keywords: Fracture · Mechanical properties · Microdeformation · Microscopy · Polymers

1. Introduction

Understanding structure–property relationships in single and multi-phase engineering polymers is central to rational attempts to meet design criteria and to develop new materials in a cost-effective way. This is increasingly important as the requirements to be satisfied simultaneously in typical applications diversify. The automotive industry provides many examples. Materials for steering wheels may need to be moulded into complex shapes whilst showing stable crack propagation up to deformation speeds typical of airbag deployment (minimizing damage to the airbag and/or the user from flying debris). Bumpers may need to be painted to match the finish of the rest of the bodywork, and so on.

Engineering polymer manufacturers and their clients make use of a range of standard tests to measure the response of

products to various types of mechanical solicitation. Although such tests may represent typical service conditions, they do not always provide broad insight into materials behaviour. The range of test speeds may be severely limited and data from different types of test are often inconsistent. This makes detailed assessment of the contribution of individual components to the mechanical properties of multiphase materials difficult. In addressing questions such as that of the role of modifier domains in the high speed tough/brittle transitions of toughened polymers, of crucial importance for bumpers, airbag envelopes, structural adhesives *etc.*, we therefore put considerable effort into:

- extending the range of conditions in which fracture mechanics parameters such as K_{IC} or G_{IC} may be determined rigorously using simple geometries, up to and beyond speeds characteristic of impact tests (K_{IC} is the *mode I plane strain critical stress intensity factor* and G_{IC} is the *mode I plane strain critical strain energy release rate* – for the present purposes we shall simply consider these to be measures of the intrinsic toughness)
- investigating whether concepts such as the essential work of fracture can

provide alternative materials parameters that reflect the intrinsic behaviour of relatively ductile polymers, for which it is difficult to obtain valid K_{IC} or G_{IC} data [1]

- developing microscopical techniques that give access to detailed information on the nature and extent of mechanically induced damage in various types of tests and materials.

Given that deformation and fracture are multi-scale phenomena, the microscopical techniques need to cover a correspondingly wide spatial range. At the same time, there should be sufficient overlap to permit incorporation of detailed but highly localized information into a global picture. This is important since at the nanometric and subnanometric levels, the structure of many polymers is still relatively poorly understood and deformation mechanisms put forward in the literature, particularly for multiphase polymers, often stem as much from hypothesis as from direct observation.

In what follows, examples of studies of microdeformation and fracture in engineering polymers will be presented, and the extent to which they provide new insight into both fundamental and practical questions will be discussed. We begin by looking at microscopical techniques and

*Correspondence: Dr. C.J.G. Plummer
Laboratoire de Polymères
Ecole Polytechnique Fédérale de Lausanne (EPFL)
CH-1015 Lausanne
Tel.: +41 21 693 28 56
Fax: +41 21 693 68 58
E-Mail: Christopher.plummer@epfl.ch

their application to model systems, with emphasis on semicrystalline polymers. We then discuss the specific example of bulk deformation in rubber toughened polymethylmethacrylates (RTPMMA) in terms of the underlying microdeformation mechanisms. Finally, we briefly consider an example of the direct application of high speed testing in an industrial context.

2. Microdeformation: Techniques and Model Studies

A large body of fundamental work on the fracture of amorphous glassy polymers has grown up over the years. Much of this has been successfully interpreted using recent micromechanical models for crack tip deformation [2] and the results of extensive studies of craze microstructures by TEM and X-ray scattering [3][4] (crazes are crack-like fibrillar damage zones characteristic of a wide range of polymers). Indeed, in some cases, a direct link can now be established between macroscopic fracture mechanics parameters and various microscopic quantities [5]. This approach is equally valid for monolithic specimens and for fracture along interfaces between different materials [6]. However, in studies of interfacial fracture, it is often relatively easy to control parameters such as the initial number of covalent bonds crossing unit area of the crack plane independently of other materials parameters. This provides a particularly attractive means of testing models involving several such parameters.

Detailed systematic observations of microdeformation in semicrystalline polymers are scarcer and quantitative micromechanical models for their behaviour are correspondingly less well developed than for amorphous glassy polymers. One of our aims has therefore been to develop direct observation by transmission electron microscopy (TEM) of crazes and craze-like structures in semicrystalline polymers as a basis for modelling deformation and fracture [7]. In amorphous glassy polymers, a convenient method of studying internal craze structures is the *in situ* deformation of films thin enough to be electron transparent. However, although this gives results consistent with those from bulk amorphous polymers [3], the situation is less clear-cut for semicrystalline polymers. Indeed it is doubtful whether one can generalize about craze microstructures in semicrystalline polymers to the same extent as in amor-

phous polymers, since their characteristic dimensions vary dramatically with the deformation conditions. This has been demonstrated in circumferentially edge notched creep specimens of high and medium density polyethylene, for example [8]. Specimens that fail after long times at low loads and high temperatures show craze fibril diameters commensurate with the crystallite spacing (of the order of 10 nm). However, specimens undergoing rapid failure at higher loads show coarse crack tip deformation zones, believed to result from rapid coalescence of local voids in the early stages of damage zone development [8]. Similar trends are seen in other semicrystalline polymers [9][10].

When the characteristic dimensions of structural elements such as spherulites or modifier particles are much larger than specimen thicknesses appropriate to TEM, the results of *in situ* thin film deformation studies are in any case difficult to extrapolate to bulk specimens. Indeed, thin films of semicrystalline polymers often show more ductile behaviour than bulk specimens, which facilitates electron diffraction studies of deformation induced phase transformations in polymers such as polyhydroxybutyrate [7], (in polyhydroxybutyrate, the phase transformation is accompanied by a change from a $4 \times 2/1$ helical conformation to a more extended $4 \times 1/1$ conformation, particularly at low temperatures). Moreover, thin film studies provide a convenient way to gain qualitative insight into microdeformation behaviour when insufficient material is available for bulk testing [11]. They also remain useful for investigating phenomena that would be difficult to observe using other methods. Thus, as shown in Fig. 1, in some cases one can observe de-

formation processes and lattice defects in thin films at the molecular level by high resolution electron microscopy (HREM) and low dose techniques [12].

Where thin film methods are inappropriate, preparation of thin sections of bulk damaged material is generally required for TEM. Although such sections are sometimes held to be difficult to prepare and prone to artefacts, the technique is relatively straightforward for semicrystalline polymers. Crack faces in specimens which have undergone a certain amount of crack propagation under the desired conditions (and whose toughness has been determined) can be wedged open under load, and the entire specimen embedded in a low viscosity epoxy or acrylate resin, with the wedge in place [10]. This permits fixing and/or staining, and thin sectioning of the damage zone in its unrelaxed state. Even in polymers unsuitable for embedding (most amorphous polymers including RTPMMA, to be discussed in the next section), it is still possible to obtain useful results by staining the specimen under load. The stain (typically RuO_4) is able to penetrate and mark those regions of the damage zone where cavitated particles and crazes form an interconnected network [13]. The same methods may be adapted for optical microscopy, scanning electron microscopy (SEM) and high-resolution field emission gun (FEG)-SEM [14]. These are particularly useful for obtaining an overview of the crack tip damage zone, enabling one to place the TEM observations, which are generally limited to relatively small regions of the specimen, in a wider context. Traditional SEM of fracture surfaces may also be informative. However, sectioning has the major advantage of allowing one to look at the whole deforma-

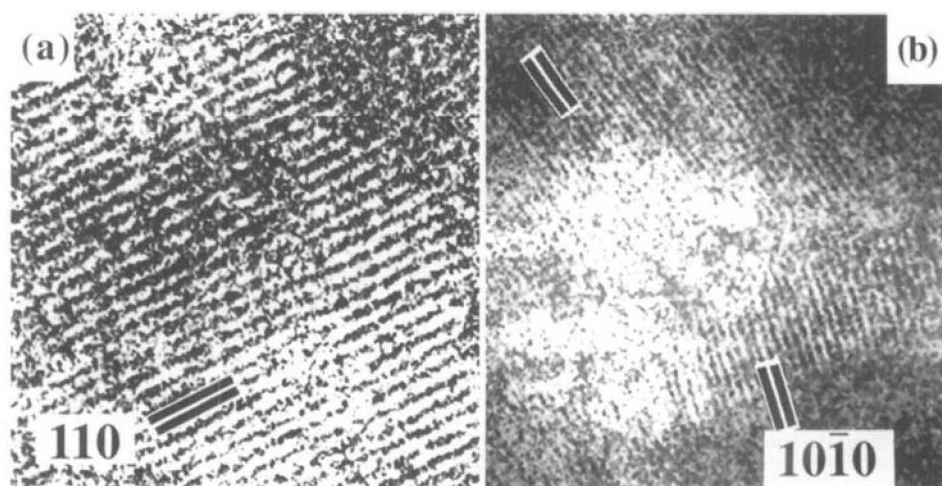


Fig. 1. HREM of (a) edge dislocations in a single melt-crystallized lamella of isotactic polypropylene (lattice spacing 0.626 nm); (b) deformation-induced twin in a friction deposited polytetrafluoroethylene film (lattice spacing 0.48 nm).

tion gradient from undeformed to fully fractured material, whereas fracture surfaces tend only to reflect the final stages of fracture.

In spite of these possibilities, the extent to which the mechanical behaviour of bonded interfaces between two immiscible semicrystalline polymers can lead to insight into their fracture behaviour has received little attention until recently. This is partly because their presumed complexity makes them unattractive for fundamental studies. Investigations of microdeformation and fracture of reaction bonded semicrystalline polyamide 6/isotactic polypropylene (PA6/iPP) interfaces nevertheless reveal remarkable similarities with amorphous polymers. The PA6/iPP interface is bonded at temperatures above the melting point of the iPP, which contains a small amount of maleic anhydride functionalized iPP that reacts with the NH_2 groups of the PA6 to form a copolymer in situ at the interface [15–17]. By varying the reaction conditions, one can vary the amount of copolymer and hence the number of covalent bonds crossing unit area of the interface, Σ . Fracture tests show the toughness, as reflected by G_{IC} to be proportional to Σ^2 , as predicted and observed for interfaces between amorphous polymers where rupture is mediated by formation of a single crack tip craze [16]. This is consistent with TEM observations of craze-like deformation zones on the iPP side of the interface (Fig. 2) and final rupture of the craze fibrils at the interface. Indeed, the observed fibril diameters of about 15 nm and reasonable estimates of parameters such as the iPP crazing stress also lead to good quantitative agreement between experimental data and model predictions [18].

When the criteria for its applicability are met, *i.e.* the existence of a single crack-tip craze, the same model accounts well for the behaviour of bulk iPP [1]. Such conditions occur during high speed ($> 1 \text{ ms}^{-1}$) fracture, for example, confirming the generality of the conclusions drawn from the interface studies. To investigate crack tip microdeformation in such cases, a limited amount of stable crack tip propagation can be assured by testing two nominally identical specimens mounted in series, so that failure of one specimen results in instantaneous unloading of the second [13][19].

At fixed Σ , the toughness also depends strongly on the draw stress associated with the crack tip damage zone. This may be demonstrated by modifying the crystal structure of iPP or by blending it

with a rubber modifier [20][21]. In rubber modified PA6/iPP bonds, G_c is directly proportional to that in unmodified PA6/iPP bonds for a given Σ [20–22]. Moreover, the constant of proportionality is close to the reciprocal of the ratio of the drawing stresses of the modified iPP and the unmodified iPP, consistent with the dependence of the toughness on draw stress anticipated for single crack tip crazes [22]. The model predictions therefore appear to be to be insensitive to the details of the architecture of the crack tip deformation zone, their validity requiring only on the existence of a localized damage zone with a constant draw stress at its boundaries. This is likely to be true not only to interfaces, but also of a wide variety of bulk materials, suggesting considerable scope for establishing direct links between the microscopic properties, microdeformation mechanisms and the bulk fracture resistance.

3. Fracture in Rubber Toughened Polymethylmethacrylate (RTPMMA)

Rubber-toughened polymers are prepared in various ways, phase separation during bulk polymerisation commonly being used in the manufacture of high-impact polystyrene, acrylonitrile-butadiene-styrene copolymers and carboxy-ter-

minated nitrile rubber toughened epoxy resins, for example. The structure of the resulting materials depends on the chemical and physical changes during polymerisation and is often difficult to control. Mixing the resin with stable pre-formed particles of different composition and size therefore provides an interesting alternative, allowing fine-tuning not only of fracture properties, but also of other properties such as optical transmission. Indeed, a strong motivation for developing RTPMMA along these lines is the exploitation of the excellent optical properties of PMMA in applications where the unmodified resin is too brittle to be of direct interest (car windows, for example). Moreover, independent control of the size, morphology and content of the modifier particles makes such materials very attractive for fundamental studies.

The RTPMMA considered here has a matrix molar mass of 130 kg/mol. As sketched in Fig. 3, the modifier consists of either a rubbery polybutylacrylate (PBA)-*co*-styrene core surrounded by a grafted PMMA shell ('two layer particles' or 2L) or a glassy core, an intermediate rubbery shell and an outer PMMA shell ('three layer particles' or 3L). The overall diameter is about 300 nm in each case. For comparison we have also looked at a 6 vol% polyurethane (PU)-PMMA interpenetrating network (IPN)

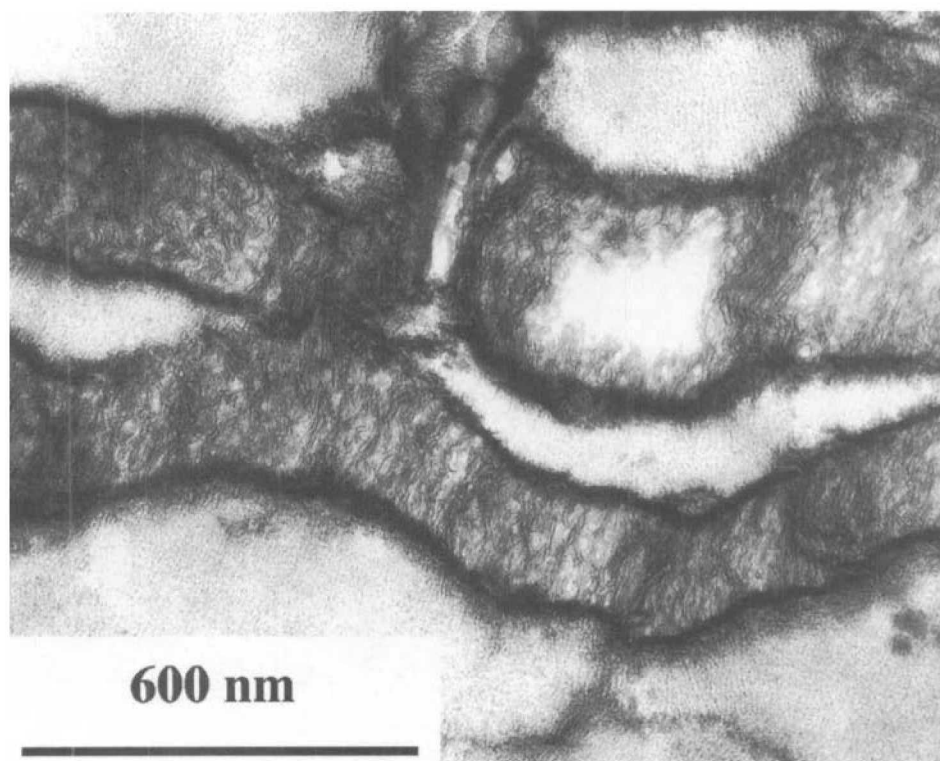


Fig. 2. Deformation in bulk isotactic polypropylene, showing craze-like structures with fibril diameters of the order of 15 nm (TEM of a RuO_4 stained thin section taken from close to a deformed polyamide 6/isotactic polypropylene interface).

in which the PMMA is highly cross-linked [23]. All these materials are transparent, but the relatively low rubber contents of the IPN and the RTPMMA containing 3L particles are advantageous from the point of view of stiffness, and toughening is also known to be more efficient with 3L particles than with 2L particles [24]. Our aim has been to explain such behaviour in terms of the role of the particles in the crack tip microdeformation mechanisms and hence to provide pointers for improving the performance of commercial RTPMMA grades.

Of paramount interest is the influence of the strain rate on the fracture toughness. Tests are therefore carried out over several decades of test speed, with the highest test speeds encompassing impact conditions (with direct relevance to final applications). These make use of a Schenk servohydraulic tensile test apparatus equipped with a remote optical extensometer [25]. Initial transient dynamic effects in the specimen are damped using a specially designed pick-up unit, allowing reliable force-displacement data to be obtained for speeds of up to 10 ms^{-1} [25]. The applicability of this method to fracture mechanics testing of pre-cracked specimens has been extensively verified from high-speed photoelasticity measurements and finite element simulations [13][26].

Results from room temperature tests on the various materials are shown in Fig. 4 [13][27][28]. Fig. 4(a) compares the performance of 30 vol% 3L particles (3L30) with that of samples containing 15, 30 and 45% of 2L particles (2L15, 2L30 and 2L45 respectively) and that of unmodified PMMA, illustrating the superior performance of the 3L particles over the whole range of test speeds investigated. All the 2L particle filled materials undergo a tough-brittle transition as impact speeds (above about 1 mms^{-1}) are approached, which is reflected by a sharp decrease in the critical stress intensity factor K_{IC} and fully unstable crack propagation. Indeed K_{IC} drops below that of the pure matrix in these grades at the highest speeds. No tough-brittle transitions are seen in either the IPN or 3L30 at high loading rates, but a tough-brittle transition does occur in 3L20 at a crosshead speed of 10 ms^{-1} , again reflected by a sharp drop in K_{IC} , as shown in Fig. 4(b). Moreover the IPN shows stable crack growth even at the highest test speeds, whereas the decrease in K_{IC} at high speeds in 3L30 is accompanied by a transition to semi-stable crack propagation. This is significant in view of our com-

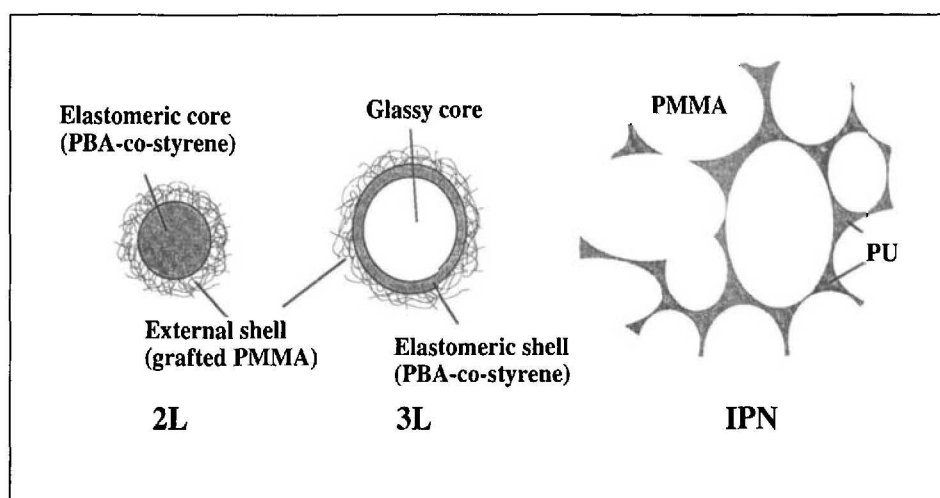


Fig. 3. Schematic representation of different RTPMMA modifier morphologies.

ments in the introduction regarding the role of unstable fracture in certain applications.

The low toughness of PMMA reflects its tendency to form a single crack tip craze during fracture at all speeds, limiting the total amount of energy dissipated

during crack propagation. In rubber toughened polymers, it is often held that stress concentrations associated with the modifier particles can increase the crack tip craze density, and that this is directly responsible for the observed increase in overall dissipation. However, relaxation

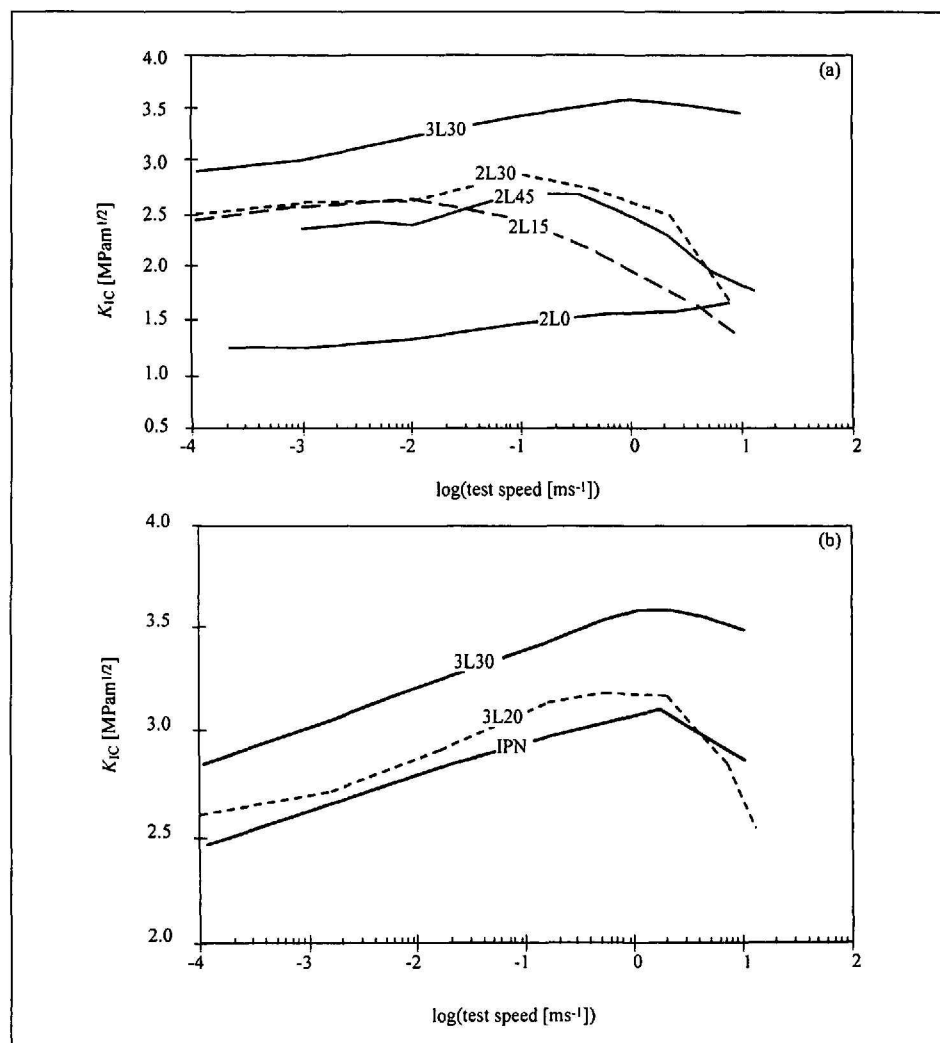


Fig. 4. Toughness, expressed in terms of the mode I plane strain critical stress intensity factor, K_{IC} , as a function of test speed in different RTPMMAs.

of local triaxial constraints as a result of particle cavitation may also trigger widespread matrix plasticity, which will again contribute to dissipation. An overview of the different stages of crack tip deformation at an intermediate test speed in 3L20 is given in Fig. 5, showing both extensive cavitation of the modifier particle shells and crazes emanating from the particles. Cavitation and crazing also appear to initiate simultaneously, *i.e.* both are present at the periphery of the damage zone shown in Fig. 5(a) (although one cannot necessarily infer a causal relationship). The crazes initially propagate perpendicular to the principal stress axis as in unmodified PMMA. However, once the crazes penetrate regions whose stress field is strongly influenced by the presence of neighbouring particles, the trajectories of the craze tips rotate towards, and link up with the (cavitated) poles of neighbouring particles, as seen in Fig. 5(b)–(d). Moreover, in the highly strained regions close to the crack tip, many of the crazes bifurcate. Thus a continuous network of voided material is created, and the accompanying triaxial constraint release is expected to favour generalized plastic flow of the matrix. The onset of unstable crack growth at higher test speeds is associated with the suppression of cavitation and multiple crazing around the crack tip, these being replaced by a single crack tip craze as in unmodified PMMA [27]. At much lower speeds cavitation and crazing are also suppressed, but here matrix plasticity is fully activated and the material is highly ductile.

An important feature of damage zones in the 3L particle toughened materials is that ligaments of rubber separate individual voids in the particle shells, linking the glass outer shell/matrix to the glassy inner core. Indeed, the particle cores become highly elongated as the crazes develop. This suggests that they continue to bear significant loads well beyond the cavitation threshold, accounting for the improved toughness compared with that of materials containing 2L particles [13][28][29]. In these latter, cavitation occurs at the particle centres, generally giving rise to large single voids, which represent points of substantial weakness at large deformations.

In the IPNs, where the matrix is crosslinked, no craze formation is observed and TEM shows that cavitation initiates in star-shaped regions of the PU rubbery phase [13][28]. The volume of the matrix elements isolated by the resulting network of voids and rubbery lig-

aments is similar that in highly deformed regions of the 3L modified PMMA. Thus, plasticity of the matrix, facilitated by release of the local triaxial constraints, may again be invoked as a dissipation mechanism. Indeed it is likely to be the only dissipation mechanism in this case, implying multiple crazing not to be a prerequisite for toughening in PMMA. However, the existence of an interconnected network of voids and/or material with a low shear modulus (either crazes or elastomer) close to the crack tip is clearly important. The mechanical response of the IPN may therefore be indicative of the important role of matrix plasticity in the particle toughened materials. Indeed, matrix plasticity has been argued to be the principal dissipation mechanism in other rubber toughened glassy polymers in which crazing is widespread [30]. It follows that the improved crack stability in the IPN may be attributed not only to the relatively low glass transition temperature of the PU, but also to the fact that the establishment of a continuous voided/rubbery network does not require

crazing, which is a highly rate dependent process.

The kinetic limitations on crazing are closely related to the interparticle distance (and hence the particle size for a given particle content) both through changes in the hydrostatic stress in the rubbery phase and through particle–particle interactions, which control the local stress in the glassy matrix. However the mobility and ultimate strength of the matrix are also important factors and given that dissipation will always ultimately depend on the matrix response, there are likely to be fundamental limits on the extent of stable crack growth at high deformation rates, regardless of the detailed behaviour. There is nevertheless considerable scope for optimising the behaviour of the particle toughened RTPMMA (which is of far greater practical interest than the IPN) through modifications in geometrical factors. This is currently being borne out by the results of ongoing development of these materials, based on the observations outlined in this section.

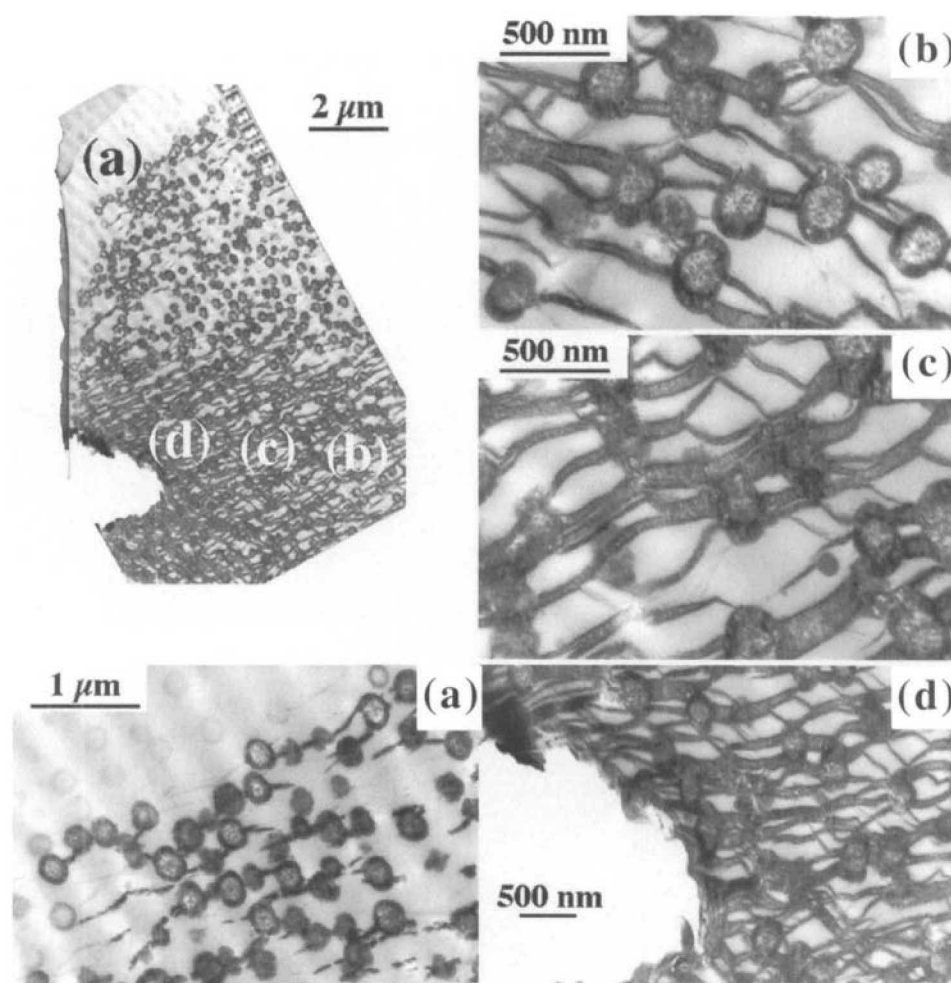


Fig. 5. TEM of deformation at the crack tip in a notched compact tensile test specimen of RTPMMA 3L20 tested at 1 mms^{-1} and stained in RuO_4 (crazes and (cavitated) rubber phase stained dark).

4. Application of High-speed Testing to Windscreen Cements

This last section describes a more practical application of high speed tensile testing in direct collaboration with an industrial partner (Sika, Switzerland). The problem is that of structural adhesives, used to fix replacement windscreen to automobiles. Strict norms are in force in the United States and elsewhere, whereby a 'safe drive away time' must be respected. This safe drive away time ensures that the adhesive will be sufficiently strong to hold the windscreen in place and, when an airbag is fitted, to support the airbag during a collision. For current adhesives, the safe drive away time is known to be sensitive to ambient humidity and temperature and extreme weather conditions can make the difference between a few hours and a day's wait for the customer. The initial aim here was to provide data allowing establishment of safe drive away times for different adhesives from numerical simulations of crash tests using finite element analysis (FEA), which were in turn to be compared with the results of real crash tests. In the FEA simulations, the bodywork, airbag and adhesive are all meshed (Fig. 6). When testing the adhesive specimen, geometries have therefore been designed to be compatible with the type of finite elements used for the simulations, so that the experimental data (generally a stress to fail as a function of speed) can be incorporated directly. Comparison of the results of such simulations with the results of the crash tests have shown excellent agreement, suggesting considerable scope for rationalizing crash testing by judicious use of simulations, thus enabling cost cutting. However, this approach also offers great promise for development, since high speed testing can

be used to test adhesives efficiently and cheaply.

5. Conclusions

The work reviewed here demonstrates the usefulness of combining rigorous bulk mechanical testing with detailed microscopic observations. In some cases, where the aim is to provide data for numerical modelling of structures, the results from bulk testing may themselves represent the basic element. However, more generally, if one requires a fundamental understanding of fracture processes, it is necessary consider elementary processes at various levels, with the eventual aim of linking fracture to the microscopic structure of the material. Although direct observation at the molecular level remains difficult, with suitable sample preparation, nanometric objects such as craze fibrils and microcrystallites are readily observable. This is not only a valuable aid in interpreting bulk phenomena, but also in defining strategies for improving bulk properties in a wide range of materials.

Acknowledgements

We gratefully acknowledge the support of Elf Atochem, Solvay, Sika, DuPont de Nemours, Ciba Speciality Chemicals and the Swiss CTI.

Received: January 15, 2001

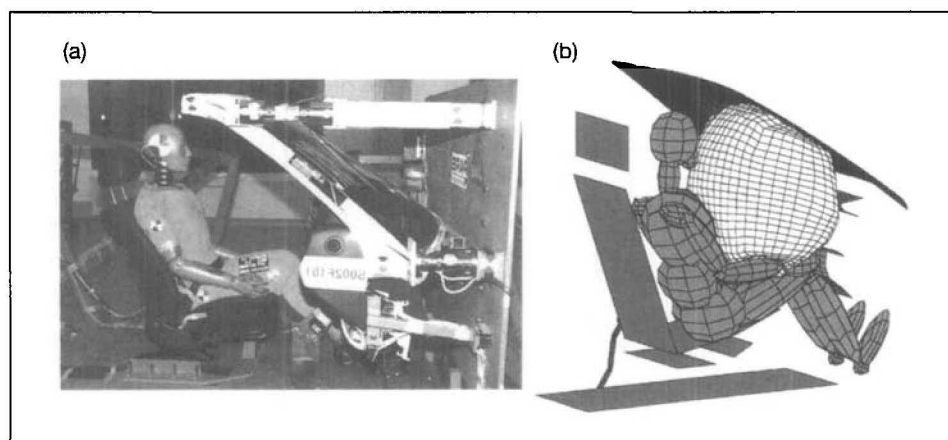


Fig. 6. (a) Crash test; (b) finite element model of the same crash test (courtesy of Sika, Switzerland).

- [1] C.J.G. Plummer, P. Scaramuzzino, R. Steinberger, R.W. Lang, H.-H. Kausch, *Poly. Eng. & Sci.* **2000**, *40*, 985.
- [2] H.R. Brown, *Macromolecules* **1991**, *24*, 2752.
- [3] E.J. Kramer, in 'Advances in Polymer Science 52/53', Ed. H.-H. Kausch, Springer Verlag, Berlin, **1983**, Ch. 1.
- [4] E.J. Kramer, L.L. Berger, in 'Advances in Polymer Science 91/92', Ed. H.-H. Kausch, Springer Verlag, Berlin, **1990**, Ch. 1.
- [5] E.J. Kramer, L.J. Norton, C.A. Dai, Y. Sha, C.-Y. Hui, *Faraday Discussions* **1994**, *98*, 31.
- [6] C. Creton, E.J. Kramer, C.-Y. Hui, H.R. Brown, *Macromolecules* **1992**, *25*, 3075.
- [7] C.J.G. Plummer, *Current trends in Polymer Science* **1997**, *2*, 125.
- [8] C.J.G. Plummer, A. Ghanem, A. Goldberg, submitted to *Polymer*.
- [9] P. Scaramuzzino, 'Analyse de la structure et de l'endommagement mécanique du polyoxyméthylène' EPFL PhD Thesis N° 1818 **1998**.
- [10] C.J.G. Plummer, P. Scaramuzzino, H.-H. Kausch, *Poly. Eng. & Sci.* **2000**, *40*, 1306.
- [11] C.J.G. Plummer, J.L. Hedrick, S. Hauert, J.G. Hilborn, H.-H. Kausch, *J. Poly. Sci.-Poly. Phys. Ed* **1996**, *34*, 2177.
- [12] C.J.G. Plummer, H.-H. Kausch, *Macromolecular Chemistry and Physics* **1997**, *198*, 485.
- [13] P. Béguelin, 'Approch expérimentale du comportement mécanique des polymères en sollicitation rapide' EPFL PhD Thesis N° 1572 **1996**.
- [14] C. Grein, EPFL PhD Thesis, **2000**.
- [15] J.-E. Bideaux, G.D. Smith, J.-A.E. Manson, C.J.G. Plummer, J.G. Hilborn, *Polymer* **1998**, *39*, 5953.
- [16] E. Boucher, J.P. Folkers, H. Hervet, L. Leger, C. Creton, *Macromolecules* **1996**, *29*, 774.
- [17] E. Boucher, J.P. Folkers, C. Creton, H. Hervet, L. Léger, *Macromolecules* **1997**, *30*, 2102.
- [18] C.J.G. Plummer, C. Creton, F. Kalb, L. Léger, *Macromolecules* **1998**, *31*, 6164.
- [19] R. Gensler, C.J.G. Plummer, C. Grein, H.-H. Kausch, *Polymer* **2000**, *31*, 3809.
- [20] C.J.G. Plummer, H.-H. Kausch, C. Creton, F. Kalb, L. Léger, *Proc. IUPAC World Polymer Congress - Macro 98, Goldcoast, Brisbane, Australia, 13-17 July, 1998*.
- [21] F. Kalb, Université Paris VI PhD Thesis, **1998**.
- [22] F. Kalb, L. Léger, C.J.G. Plummer, C. Creton, P. Marcus, submitted to *Macromolecules*.
- [23] P. Heim, C. Wrotecki, M. Avenel, P. Gaillard, *Polymer* **1993**, *34*, 1653.
- [24] P.A. Lovell, *Trends in Polymer Science* **1996**, *4*, 264.
- [25] P. Béguelin, M. Barbezat, H.-H. Kausch, *J. Phys. III France* **1991**, *1*, 1867.
- [26] P. Béguelin, C. Fond, H.-H. Kausch, *Int J. Fract.* **1998**, *89*, 85.
- [27] C.J.G. Plummer, P. Béguelin, H.-H. Kausch, *J. Colloids and Interfaces A* **1999**, *153*, 551.
- [28] P. Béguelin, C.J.G. Plummer, H.-H. Kausch, H.-H. in 'Polymer Blends and Alloys', Ed. G.O. Shonaike, G.P. Simon, Marcel Dekker, NY **1999**, Ch 19.
- [29] C.J.G. Plummer, P. Béguelin, H.-H. Kausch, *Polymer* **1996**, *37*, 7.
- [30] A.M.L. Magalhães, R.J.M. Borggreve, *Macromolecules* **1995**, *28*, 5841.